

## **Supporting Information**

Ammonium ion pre-intercalated MnO<sub>2</sub> on carbon cloth for high energy  
density asymmetric supercapacitor

Chaoyi Zheng, Xiaohong Sun<sup>\*</sup>, Xinqi Zhao, Xi Zhang, Jiawei Wang, Zhuang Yuan,  
Zhiyou Gong

*Key Laboratory of Advanced Ceramics and Machining Technology of Ministry of  
Education, School of Materials Science and Engineering, Tianjin University, Tianjin  
300072, China*

<sup>\*</sup>Corresponding author.

*E-mail address:* sunxh@tju.edu.cn

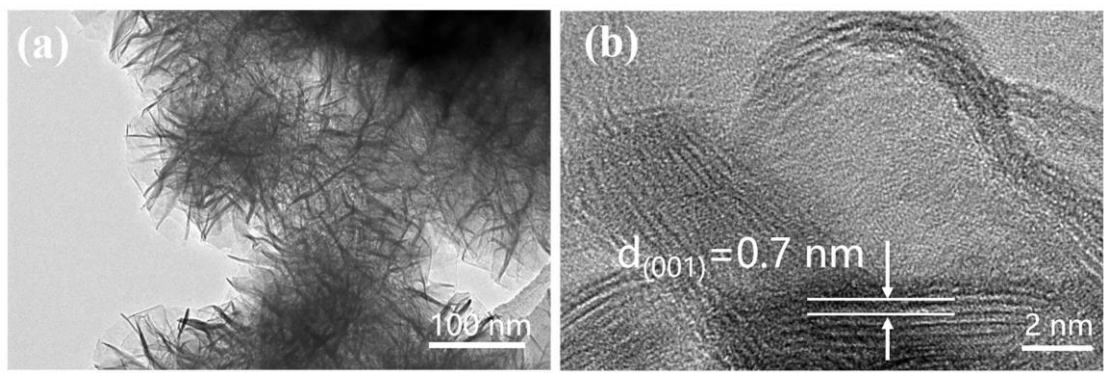


**Figure S1.** (a) TEM image of CC@NMO, (b) HRTEM image of CC@NMO.

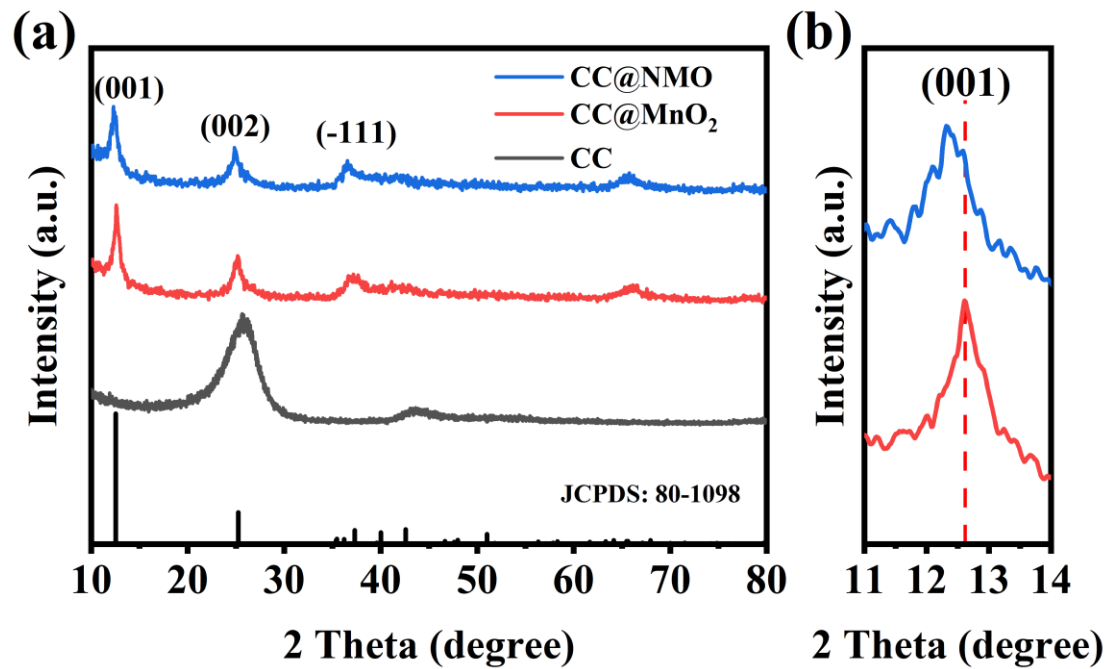


**Figure S2.** XRD patterns of CC@NMO, CC@MnO<sub>2</sub> and CC.

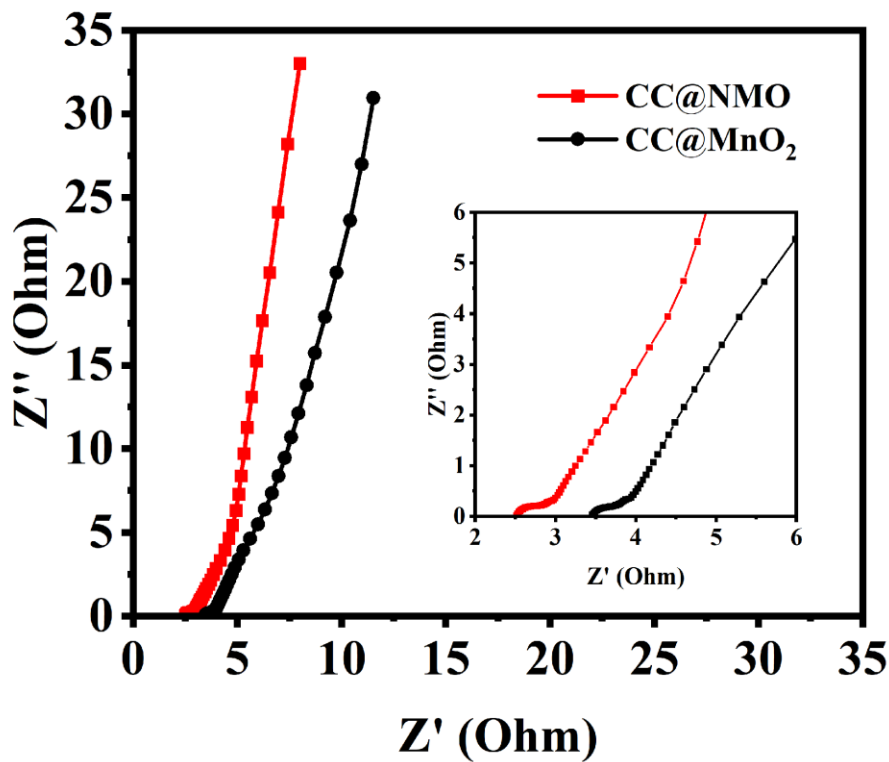


**Figure S3.** EIS curves of CC@NMO and CC@MnO<sub>2</sub>.

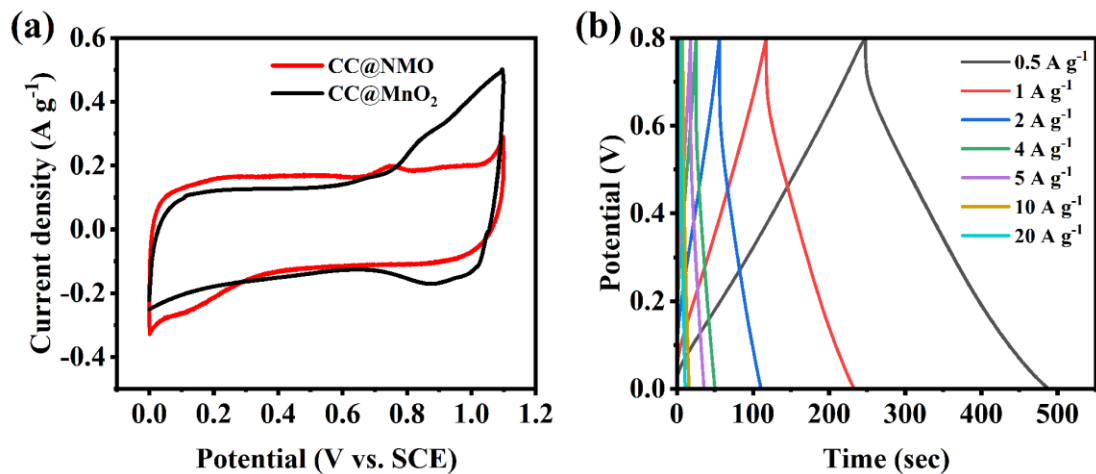


**Figure S4.** (a) comparison of CC@NMO and CC@MnO<sub>2</sub> at 1 mV s<sup>-1</sup> at 0-1.1 V, (b)

GCD curves of CC@MnO<sub>2</sub> at 0-0.8 V at different current densities.

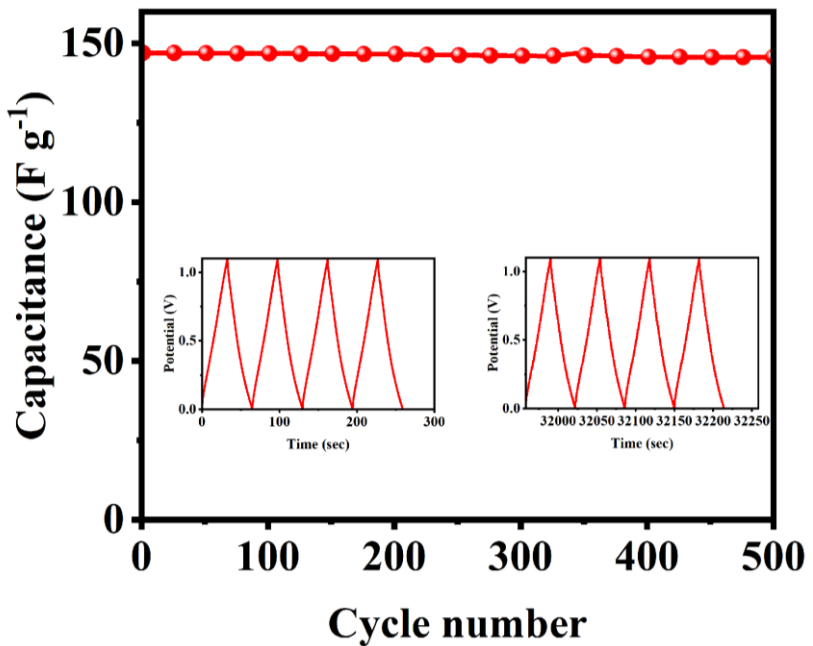


**Figure S5.** cycle stability of CC@NMO at  $5 \text{ A g}^{-1}$ .

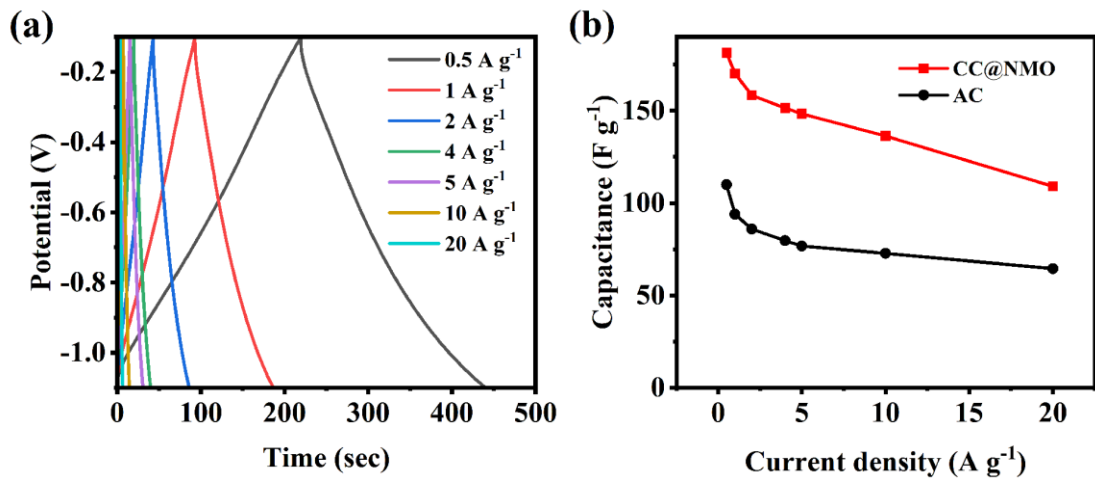


**Figure S6.** (a) GCD curves of AC at -0.1 to -1.1 V at different current densities, (b) Capacitance of CC@NMO and AC at different current densities.

**Table S1.** Comparison of energy density and power density with other recent studies.

Sample	Energy density	Power density	References
	(Wh/kg)	(W/kg)	
<b>CC@NMO</b>	<b>63.49</b>	<b>949.8</b>	<b>This work</b>
MnO <sub>2</sub> @PCN//PCN	31.13	193.6	[42]
N/P-HCS@MnO <sub>2</sub> -30	32.21	449.8	[43]
G/MnO <sub>2</sub>	19.6	351	[44]
MnO <sub>2</sub> @SnO <sub>2</sub> //AC	18.05	403.6	[45]
MnO <sub>2</sub> @N-APC//N-APC	28	506	[46]
AC//MnO <sub>2</sub> @NH <sub>4</sub> MnF <sub>3</sub>	11.2	1000	[47]
MnO <sub>2</sub> /SHAC-3//SHAC	48.2	98.5	[48]
Co-Ni LDH/MC973	37	750	[49]
Ni-Co LDH-3	21.28	500	[50]
NCNS–NCW	56.1	349	[51]

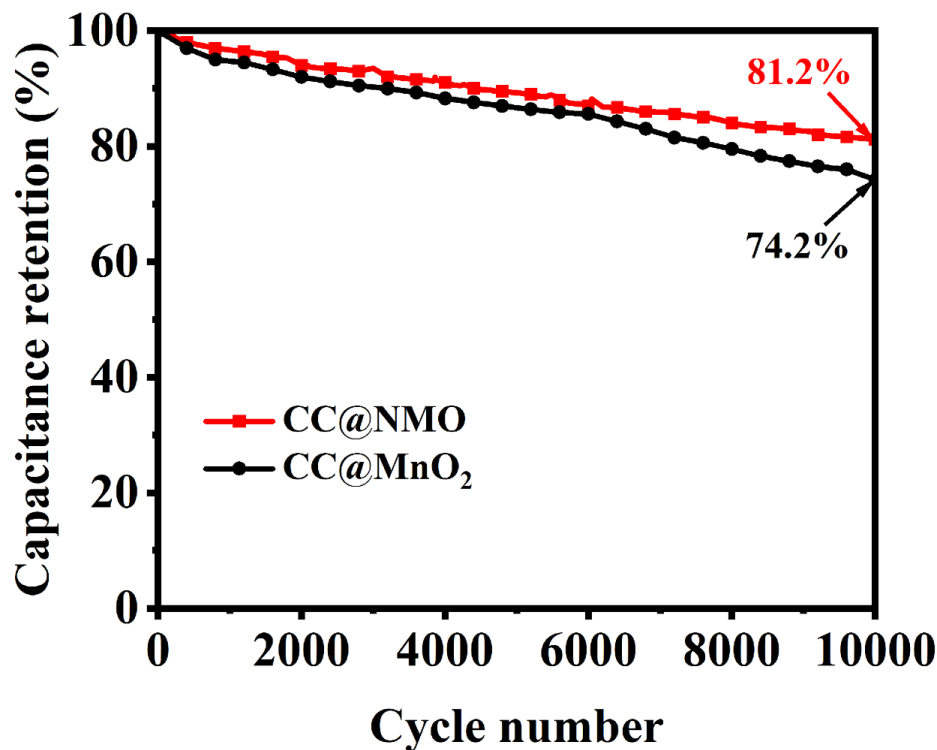


**Figure S7.** Comparison of cycle stability of CC@NMO//AC and CC@MnO<sub>2</sub>//AC.

## References

42. Feng, W.C.; Liu, G.; Wang, P.P.; Zhou, J.W.; Gu, L.X.; Chen, L.Z.; Li, X.Y.; Dan, Y.Y.; Cheng, X.F. Template Synthesis of a Heterostructured MnO<sub>2</sub>@SnO<sub>2</sub> Hollow Sphere Composite for High Asymmetric Supercapacitor Performance. *ACS Appl. Energy Mater.* **2020**, *3*, 7284-7293, doi:10.1021/acsaem.0c00388.
43. Li, B.; Zhang, X.H.; Dou, J.H.; Zhang, P.X. Construction of MnO<sub>2</sub>@NH<sub>4</sub>MnF<sub>3</sub> core-shell nanorods for asymmetric supercapacitor. *Electrochim. Acta* **2020**, *347*, doi:10.1016/j.electacta.2020.136257.
44. Li, D.Y.; Lin, J.; Lu, Y.; Huang, Y.; He, X.; Yu, C.; Zhang, J.; Tang, C.C. MnO<sub>2</sub> nanosheets grown on N-doped agaric-derived three-dimensional porous carbon for asymmetric supercapacitors. *J. Alloys Compd.* **2020**, *815*, doi:10.1016/j.jallcom.2019.152344.
45. Tan, Y.L.; Yang, C.X.; Qian, W.W.; Teng, C. Flower-like MnO<sub>2</sub> on layered carbon derived from sisal hemp for asymmetric supercapacitor with enhanced energy density. *J. Alloys Compd.* **2020**, *826*, doi:10.1016/j.jallcom.2020.154133.
46. Wu, P.C.; Gao, M.; Yu, S.C.; Feng, M.L.; Liu, S.H.; Fu, J.W. MnO<sub>2</sub> nanosheets grown on N and P co-doped hollow carbon microspheres for high performance asymmetric supercapacitor. *Electrochim. Acta* **2020**, *354*, doi:10.1016/j.electacta.2020.136681.
47. Yang, Y.K.; Niu, H.; Qin, F.F.; Guo, Z.Y.; Wang, J.S.; Ni, G.S.; Zuo, P.P.; Qu, S.J.; Shen, W.Z. MnO<sub>2</sub> doped carbon nanosheets prepared from coal tar pitch for advanced asymmetric supercapacitor. *Electrochim. Acta* **2020**, *354*, doi:10.1016/j.electacta.2020.136667.
48. Zhang, M.; Zheng, H.; Zhu, H.L.; Xu, Z.F.; Liu, R.; Chen, J.L.; Song, Q.; Song, X.J.; Wu, J.; Zhang, C.Z.; et al. Graphene-wrapped MnO<sub>2</sub> achieved by ultrasonic-assisted synthesis applicable for hybrid high-energy supercapacitors. *Vacuum* **2020**, *176*, doi:10.1016/j.vacuum.2020.109315.
49. Wang, M.; Feng, Y.; Zhang, Y.; Li, S.S.; Wu, M.M.; Xue, L.L.; Zhao, J.H.; Zhang, W.; Ge, M.Z.; Lai, Y.K.; et al. Ion regulation of hollow nickel cobalt layered double hydroxide nanocages derived from ZIF-67 for High-Performance supercapacitors. *Appl. Surf. Sci.* **2022**, *596*, doi:10.1016/j.apsusc.2022.153582.
50. Yang, J.J.; Li, H.L.; He, S.J.; Du, H.J.; Liu, K.M.; Zhang, C.M.; Jiang, S.H. Facile Electrodeposition of NiCo<sub>2</sub>O<sub>4</sub> Nanosheets on Porous Carbonized Wood for Wood-Derived Asymmetric Supercapacitors. *Polymers* **2022**, *14*, doi:10.3390/polym14132521.
51. Yao, Y.S.; Li, H.J.; Yu, Y.; Du, C.; Wan, L.; Ye, H.; Chen, J.; Zhang, Y.; Xie, M.J. Stabilizing microstructure of Co-Ni layered double hydroxides by magnesium doping and confinement in carbonaceous mesopores for ultrahighly-stable asymmetric supercapacitor. *J. Energy Storage* **2023**, *59*, doi:10.1016/j.est.2022.106422.